Optimization of parameters and imaging techniques within the field of MRI

Marijn van Dam and Stan de Haas*
Applied Physics, Delft University of Technology
(Dated: November 25, 2024)

This report investigates the application of a Fabry-Pérot interferometer for the optical characterization of cantilever beams and a piezo-driven displacement system. The interferometer measured resonance frequency shifts caused by beam vibrations and piezo-stack activations. The goal of the research included determining the responsivity of cantilevers of different length and determining if theoretical predictions in the field of optomechanics match measurements. The responsivity of the optical cavity was calculated to be $R = 1.4 \pm 0.27\ \frac{\mu m}{V}$ and the cutoff frequency of the piezo-stack was calculated as $1125 \pm 125 Hz$. However, inconsistencies between theoretical calculations and experimental resonance frequencies suggest possible inaccuracies in beam dimensions or limitations in equipment. These findings highlight both the challenges and potential improvements in using interferometric techniques for mechanical and optical system characterization.

I. INTRODUCTION

Mechanical oscillators are useful instruments in physics and engineering, they are tools to better understand the dynamics of systems from macro to quantum [1]. The oscillation within a system gives information about its properties and can be an indicator of time. In optomechanics, light is used as a measurement of mechanical motion. The basic setup for this optomechanics research involves an optical cavity in which the mechanical oscillator affects the type of interference between the light leading to resonance frequencies or on the other hand destructive interference. This change can be detected by measuring the difference in the intensity of the light. By using a piezo-stack as mechanical oscillator this research will attempt to classify cantilever beams, calculate the responsivity of the system and determining the cutoff frequency. The cantilevers are classified by looking at how these microscopic beams move and how light interacts with them using a Fabry-Pérot interferometer. The cantilever beams, made from a type of glass called silicon nitride, are controlled by a piezo-stack. The piezo-stack varies in deflection due to an electrical signal. This research paper studies how the beams vibrate at different frequencies and how well the piezo-stacks respond to changes in voltage. The goal of this part of research is to compare these results with theoretical predictions and figure out where the experimental setup might need improvement. In order to do this, the research starts by characterizing the optical cavity, the responsivity of the piezo-stack and finds the resonance frequencies of the cantilevers.

By testing how the piezo-stack performs, more was found out about its features. This report highlights both the successes and difficulties of this experiment, hoping to improve understanding of how these systems work and how they can be made more precise.

* m.j.vandam@student.tudelft.nl
s.s.f.dehaas@student.tudelft.nl

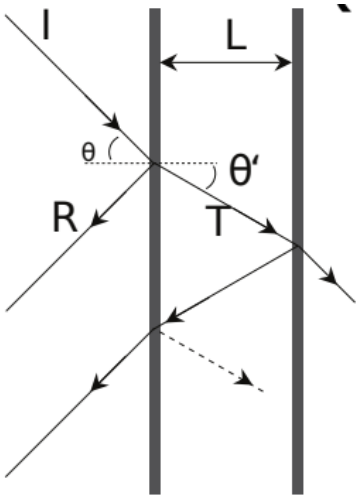

FIG. 1: The principle of a Fabry-Pérot interferometer.

II. THEORY

Fabry-Pérot interferometer

An interferometer is a device that measures the interference of two beams of light. There are several types of interferometers, this experiment uses a Fabry-Pérot interferometer. In this type of interferometer, part of a light source is reflected by a reflective surface while some of the light passes through, where it gets reflected by a second surface. This second surface is usually the object that is being studied. The light reflected by the second surface then interferes with the light reflected by the first surface. Depending on the distance L between the surfaces (referred to as the cavity length) and the wavelength λ, the interference is constructive or destructive. Figure 1 provides a schematic representation of this concept.

In this experiment, the tip of the optical fiber serves as the semi-reflective surface, while the surface of the chip serves as the second, reflective surface. The transmitted light beams can be reflect multiple times between the

semi-reflective surface and the second surface before re-entering the fiber and interfering with the other beams, as shown in Figure 1. The part where the light beams get reflected back and forth is known as the cavity. If the two reflective surfaces are separated by a distance L, the optical path difference of the light beams is given by:

$$\Delta L = 2nL\cos\Theta \tag{1}$$

where n is the refractive index of the medium between the mirrors (this is air in our experiment, which gives $n \approx 1$, and Θ is the angle of refraction. The phase difference δ of the light with wavelength λ is then equal to:

$$\delta = \frac{4\pi}{\lambda} nL\cos\Theta \tag{2}$$

To determine whether interference is constructive or destructive, equation 2 is analyzed. Constructive interference occurs when the phase difference equals an integer multiple of wavelengths, expressed as $\delta = m\lambda$, where m is an integer. Destructive interference occurs when the phase difference is an odd multiple of half a wavelength, expressed as $\delta = \left(m + \frac{1}{2}\right)\lambda$, where m is an integer. Substituting these conditions into equation 2, the expressions for L are obtained. For constructive interference:

$$L = \frac{m\lambda}{4\pi n\cos\Theta} \tag{3}$$

and for destructive interference:

$$L = \frac{\left(m + \frac{1}{2}\right)\lambda}{4\pi n\cos\Theta} \tag{4}$$

Using equation 1 in equations 3 and 4, the expressions simplify to:

$$\text{Constructive interference: } L = \frac{m\lambda}{2}, \tag{5}$$

$$\text{Destructive interference: } L = \frac{\left(m + \frac{1}{2}\right)\lambda}{2}, \tag{6}$$

where $m = 0, 1, 2, 3, \ldots$

Beam mechanics

On the chip four cantilevers are fixed, two of 200 μm and two of 100 μm. This section explores the mechanical behavior of these cantilevers, which consist of rectangular silicon nitride beams. Their motion is described by the Euler-Bernoulli equation, which looks like:

$$EI_z \frac{\partial^4 Z(x,t)}{\partial x^4} + \rho A \frac{\partial^2 Z(x,t)}{\partial t^2} = 0. \tag{7}$$

Here:

- ρ is the material density (3440 kg/m^3),
- $A = wh$ is the cross-sectional area of the beam ($w = 20$ μm, $h = 0.5$ μm),
- E is the Young's modulus ($285 \cdot 10^9$ Pa),
- I_z is the area moment of inertia, calculated by: $I_z = \int_A Rz^2\, dA = \int_0^w R\, dy \int_{-h/2}^{h/2} z^2\, dz = [y]_0^\omega [z^2/3]_{-h/2}^{h/2} = \frac{wh^3}{12}$

It may be assumed that that $Z(x,t)$ can be expressed as follows:

$$Z(x,t) = u(x)e^{i\omega t}, \tag{8}$$

substituting this into the Euler-Bernoulli equation, gives that:

$$u''''(x) - k^4 u(x) = 0 \text{ where } k^4 = \frac{\rho A\omega^2}{EI_z} \tag{9}$$

A. General solution and boundary conditions

In order to be able to solve the general solution to the ordinary differential equation 9:

$$u(x) = a_1\cosh(kx) + a_2\sinh(kx) + a_3\cos(kx) + a_4\sin(kx) \tag{10}$$

their must be (at least) four boundary conditions (BCs), since there are four unknown parameters. At the fixed end ($x = 0$) we have $u(0) = 0$ (1) and $u'(0) = 0$ (2). This is the case at the fixed the cantilever is unable to move so $u(0) = 0$, this also results in the fact that it is not able to have a velocity since its position is fixed, so $u'(0) = 0$. The other two BCs follow from the fact that respectively the bending moment and shear force are zero at the free end. This results in $u''(L) = 0$ (3) and $u'''(L) = 0$ (4) [2]. In order to solve for $a_1 - a_4$, the derivatives of the general solution for $u(x)$ are needed. This gives:

$u(x) = a_1\cosh(kx) + a_2\sinh(kx) + a_3\cos(kx) + a_4\sin(kx)$

$u'(x) = a_1 k\sinh(kx) + a_2 k\cosh(kx) - a_3 k\sin(kx) + a_4 k\cos(kx)$

$u''(x) = a_1k^2\cosh(kx)+a_2k^2\sinh(kx)-a_3k^2\cos(kx)-a_4k^2\sin(kx)$

$u'''(x) = a_1k^3\sinh(kx)+a_2k^3\cosh(kx)+a_3k^3\sin(kx)-a_4k^3\cos(kx)$

BC 1 gives that $a_1 + a_3 = 0$ and BC 2 gives that $a_2 + a_4 = 0$. BC 3 together with $a_1 = -a_3$ and $a_2 = -a_4$ gives that $a_3(\cosh(kL) + \cos(kL)) + a_4(\sinh(kL) + \sin(kL)) = 0$. BC 4 together with $a_1 = -a_3$ and $a_2 = -a_4$ gives that $a_3(\sinh(kL) - \sin(kL)) + a_4(\cosh(kL) + \cos(kL)) = 0$. Since the trivial solution is not wanted, the determinant of the following matrix must be zero:

$$\begin{bmatrix}\cosh(kL)+\cos(kL) & \sinh(kL)+\sin(kL)\\ \sinh(kL)-\sin(kL) & \cosh(kL)+\cos(kL)\end{bmatrix}\begin{bmatrix}a_3\\ a_4\end{bmatrix}$$

Calculating the determinant we find $\cosh^2(kL) + \cos^2(kL)+2\cosh(kL)\cos(kL)-\sinh^2(kL)+\sin^2(kL)$. Using the identity $\sin^2(x) + \cos^2(x) = 1$ and $\cosh^2(x) - \sinh^2(x) = 1$ we find that $1+\cosh(kL)\cos(kL) = 0$ so for $\alpha_n = k_nL = kL$ we see that $1 + \cosh(\alpha_n)\cos(\alpha_n) = 0$ is valid for arbitrary numbers of L.

B. Numerical solution for α_n

Using numerical methods, the first ten roots of α_n can be seen in table I. A complete description of how this is done can be found in [3].

Mode (n)	$\boldsymbol{\alpha_n}$
1	1.875
2	4.694
3	7.855
4	10.996
5	14.137
6	17.279
7	20.420
8	23.562
9	26.706
10	29.845

TABLE I: Table that gives the corresponding α_n for every mode.

Using the found values for α_n and the facts that if $a_3 = C$, $a_1 = -a_3 = -C$, $a_4 = -a_3 \cdot \frac{\cosh(kL)+\cos(kL)}{\sinh(kL)+\sin(kL)} = -C\frac{\cosh(\alpha_n)+\cos(\alpha_n)}{\sinh(\alpha_n)+\sin(\alpha_n)}$ and $a_2 = -a_4 = C\frac{\cosh(\alpha_n)+\cos(\alpha_n)}{\sinh(\alpha_n)+\sin(\alpha_n)}$, it is possible to determine the mode shape for every α_n using the found values for $a_1 - a_4$ and equation 10. The mode shape for the first four modes can be seen in figure 2. Here, C is chosen to be -1. However, any other value for C would results in the same shape as it is a constant.

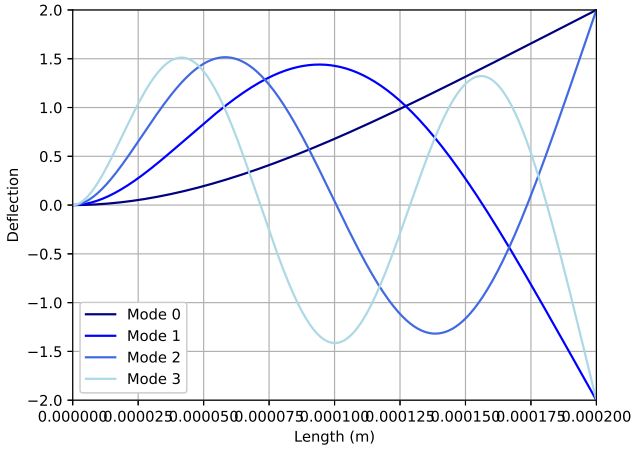

FIG. 2: Plot that gives the relation between Length (x) and deflection for the 200 μm cantilever. For the first four modes found in table I. It is chosen that $a_3 = 1$, which only influences the amplitude, not the shape.

C. Resonance frequencies

The resonance frequency f_n for the cantilevers can be calculated using 9, $\alpha_n = k_nL$, $f = \frac{\omega}{2\pi}$ and earlier relations given below equation 7. This gives:

$$f_n = \frac{\alpha_n^2}{2\pi}\sqrt{\frac{Eh^2}{12\rho L^4}} \tag{11}$$

Substituting the dimensions ($w = 20\,\mu$m, $h = 0.5\,\mu$m) and lengths ($L_1 = 100\,\mu$m, $L_2 = 200\,\mu$m), the first five resonance frequencies are calculated (see II.

Mode (n)	$\boldsymbol{\alpha_n}$	$\boldsymbol{f_n}$ **(kHz) for** L_1	$\boldsymbol{f_n}$ **(kHz) for** L_2
1	1.875	73.518	18.379
2	4.694	460.729	115.182
3	7.855	1290.055	322.514
4	10.996	2527.993	631.998
5	14.137	4178.954	1044.783

TABLE II: Resonance frequencies for the first five modes for both the 100 μm and the 200 μm cantilever.

III. METHOD

The idea of the research is simple. In order to calculate the resonance frequencies of the cantilever beams, one sends a ray of light to the beam. The ray gets reflected and send to a photo-diode which converts the intensity of the light to an electrical signal.

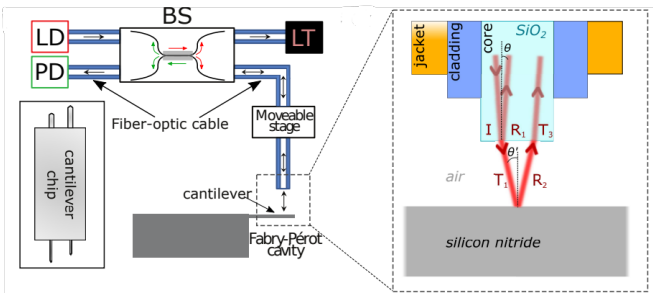

FIG. 3: A schematic overview of the setup

In the figure above you can see the full setup. The laser-diode (LD) sends a light signal through an optical fiber to a 50:50 beamsplitter (BS). Half of the light is sent to the light trap (LT) and the other half is sent to the movable stage which can be aimed at the cantilever chip. Part of the incoming reflects of the glass of the fiber, and the rest is transmitted (T1). The cantilever chip then reflects the transmitted light to the fiber tip (T2). The light gets reflected back through the optical fiber to the photo-diode and transfers this to an electrical signal which can be read by an oscilloscope or spectrum analyzer.

A. Characterization of the optical cavity

The first step is to find out what the optical cavity is. The goal is to relate the movement of the piezo-stack, which functions as a mirror, to the electrical signal. Start the measurement with a triangular wave of $10 - 50\ Hz$ and point the tip of the fiber as close as possible to the center of the chip and then bring the fiber tip back approximately the diameter of the tip. To do this, a microscope is used. Now the oscilloscope displays the signal generator and the photo-diode signal. One can see how many peaks there are per voltage to calculate the responsivity with equation 12.

$$R = \frac{\Delta L}{\Delta V} = \frac{(n-1)\frac{\lambda}{2}}{\Delta V} \tag{12}$$

ΔV is the difference between the driving signal and the photo-diode signal and λ is the wavelength of the light. In this experiment $\lambda = 635\ nm$ is used.

B. Cutoff frequency

Another goal of this experiment is also to determine the cutoff frequency of the piezo amplifier. The frequency at which the output of the amplifier reduces by a factor of 2 (or -3 dB) is called the cutoff frequency. The result of this will be a sudden drop in amount of peaks in a trace at a certain frequency. Thus one can determine the cutoff frequency by looking at the oscilloscope at different frequencies and seeing where this change occurs.

C. Detection of resonance motion

The next goal of the experiment is to determine the resonance frequencies of the two different cantilevers attached to the chip. The oscilloscope get replaced for a spectrum analyzer. A spectrum analyzer is used to measure the strength of photo-diode signal for different frequencies in a certain domain. The spectrum analyzer also features a tracking generator which allows it to drive a signal. By using the tracking generator one can measure a driven frequency of response of a cantilever. In order to determine the resonance frequency the piezo-stack gets replaced by a dither-piezo. A dither-piezo is smaller but operates on a wider range of frequencies.

Start by setting the function on the analyzer to a sine-wave between 15 and 45 kHz. An attempt was made to try to reach a peak-to-peak amplitude of $15 - 20V$ but because of the impedance of the circuit this was not possible for these higher frequencies, so $5-10V$ was used. The tip of the fiber remains directed towards the center of the chip.

With this setup working, set the tracking generator to drive from 1 kHz to 50 kHz. The effect of changing the frequency and voltage is then studied, with traces being recorded.

On each side the chip there are two cantilever beams, one of length 200 μm and one of length 100 μm. The movable stage is set to aim the fiber tip at the end of the cantilever beams. Then use the tracking generator to sweep the driving frequency of the dither-piezo. On the spectrum analyzer it is possible to see if there is an amplitude peak at a certain frequency. In order to best see this one can lower the bandwidth. Additionally, the fiber tip can be moved along the beam relate amplitude to length of the cantilever. Then one can save all these traces for data analysis.

IV. RESULTS AND DISCUSSION

A. Responsivity

In order to calculate the responsivity of the piezo-stacks four traces were made which can be found in the appendix (see figure 10-13). Respectively for a triangular input signal of $2, 3, 4$ and $5\ V$.

A computer algorithm is used to find the peaks found in these traces. Then, the distance and difference in input voltage between the peaks can easily by calculated. Afterwards, by using formula 12, one can calculate the responsivity (R) at different voltages. Since this is done for many peaks, for each voltage the uncertainty can be calculated by calculating the standard deviation for all the found values of R. A more detailed description, all data and the plots can be found in [3]. A plot of the found values for R and is displayed in figure 4.

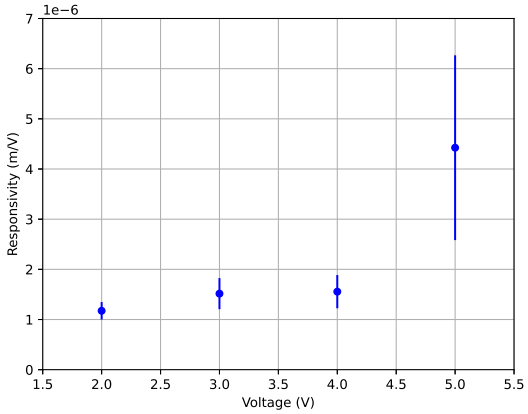

FIG. 4: Plot that gives the relation between the voltage (V) and the found values for the responsivity (m/V) including its uncertainty.

The responsivity seems to lie on a straight line except for the trace at $5\ V$. The uncertainty here is also way higher. This problem can be explained by the fact that as the voltage increases the frequency increases. These very short period could lead to the piezo-stack not responding fast enough. For this reason the trace for $5\ V$ is removed and it can thus be calculated that $R = 1.4 \pm 0.27\ \frac{\mu m}{V}$.

In a further research one could try to make more scans at low voltage or to use piezo that better responds to the short periods in order to increase the accuracy of the responsivity.

B. Cutoff frequency

As described in III B, different frequencies can be scanned to try and find the point where the output of the amplifier reduces by a factor of two. In the case of this experiment this point is found to be between 1000 and 1250 Hz. One can see the difference in the traces in figure 5. Thus the cutoff frequency is $1125 \pm 125 Hz$.

This a very large inaccuracy, which stems from the fact that at first it was thought that the cutoff frequency was between 1250 and 1260 Hz. This lead to many traces being made at the wrong frequency.

Because there is being looking in a interval of this $250\ Hz$ small issues in the equipment could also go unnoticed. Future research could involve scanning a broader range with smaller distances in between them to increase the accuracy. Employing different measurement techniques or instruments could also help validate these findings.

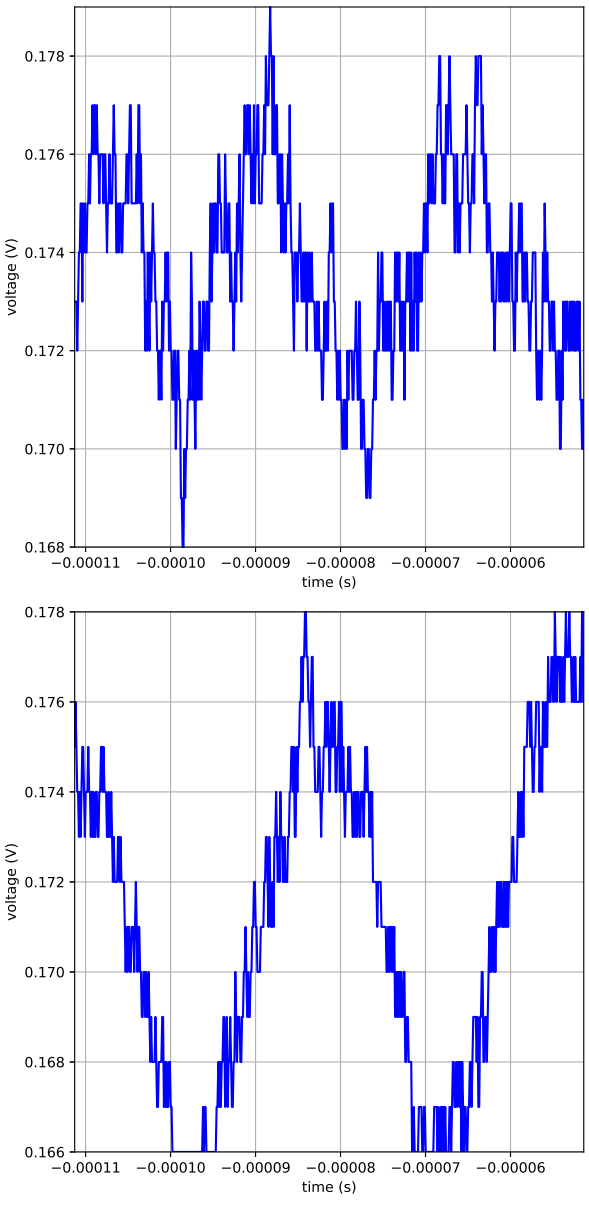

FIG. 5: Trace for peak to peak for respectively 1000 and 1250 Hz

C. Resonance frequencies

This section aims to measure the resonance peaks and study their behavior. Firstly, the effect of voltage and frequency change is studied. Afterwards the resonance peaks of the two cantilevers are measured. Lastly, a few resonance modes are mapped out.

First, figure 6 shows the relation between the frequency and amplitude for different frequencies set into the signal generator. From this it can easily be seen that the resonance peaks occur at the set frequencies in the generator. An other phenomenon that can be seen is the fact that the amplitude decreases when increasing the frequency. In the experiment the output voltage was set a constant 10 V, however, due to fact the high frequencies lead to a lower resistance, since $Z = 1/\omega C$. the generator was not able to output this 10 V and outputted a lower voltage (otherwise the current would become to big). This decrease in voltage as frequencies rise can be seen in the label of figure 6. So the decrease in amplitude can be ascribed to the decrease in voltage.

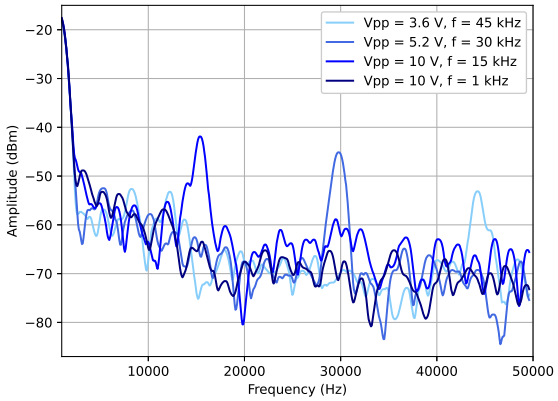

FIG. 6: Plot that gives the relation between the frequency (Hz) and amplitude (dBm) for four different frequencies in the set to the signal generator.

Secondly, for both the 200 μm and 100 μm cantilever the resonance peaks were measured out in the in the $0-100$, $0-400$ and $0-1600$ kHz ranges, see respectively figure 7 and figure 8. In both cases two different measurements were made to increase the accuracy and validity of this research. This paper starts of by analyzing the results for the 200 μm cantilever.

From figure 7 it follows that there are peaks at $14, 88$ and 240 kHz. By looking at figure 7 and the theoretical values deduced in table II, it is observed that these values do not match the theoretical values. However, all values are equal relative distance away from there theoretical values. Therefore the error has a linear correlation with the frequency. Looking at 11 f_n only has linear relation the h, therefore h might be inaccurate and actually be a lower value. During the experiment it was also found that fiber tip was not clear and accurate. Therefore higher resonance peaks, with a lower amplitude, were not measured. This might also have affected the inaccurate measurements in the peaks that were found.

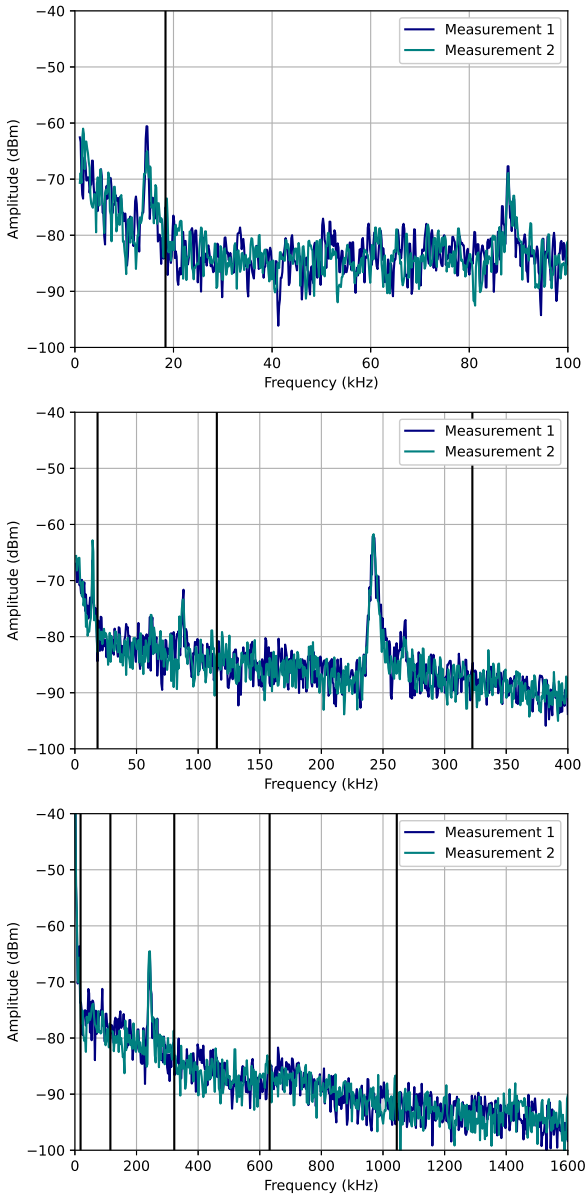

FIG. 7: Plot that gives the relation between the frequency (kHz) and amplitude (dBm) measured twice in the frequency domains $1-100$, $1-400$ and $1-1600$ kHz for the 200 μm cantilever. Additionally, the theoretically found resonance frequencies (see table II) are plotted.

From figure 8 it follows that there is a peak at 52 kHz for the 100 μm cantilever. This peak does not match the theoretical value in table II. Since only one peak was measured it is hard to specify this error. However, the relative error seems to align with the one found for the 200 μm cantilever. It could therefore be of the same type.

The fact that other resonance peaks were not found might have to do with the poor fiber tip and the fact that for a smaller cantilever it is harder to map out the resonance peaks since they occur at higher frequencies.

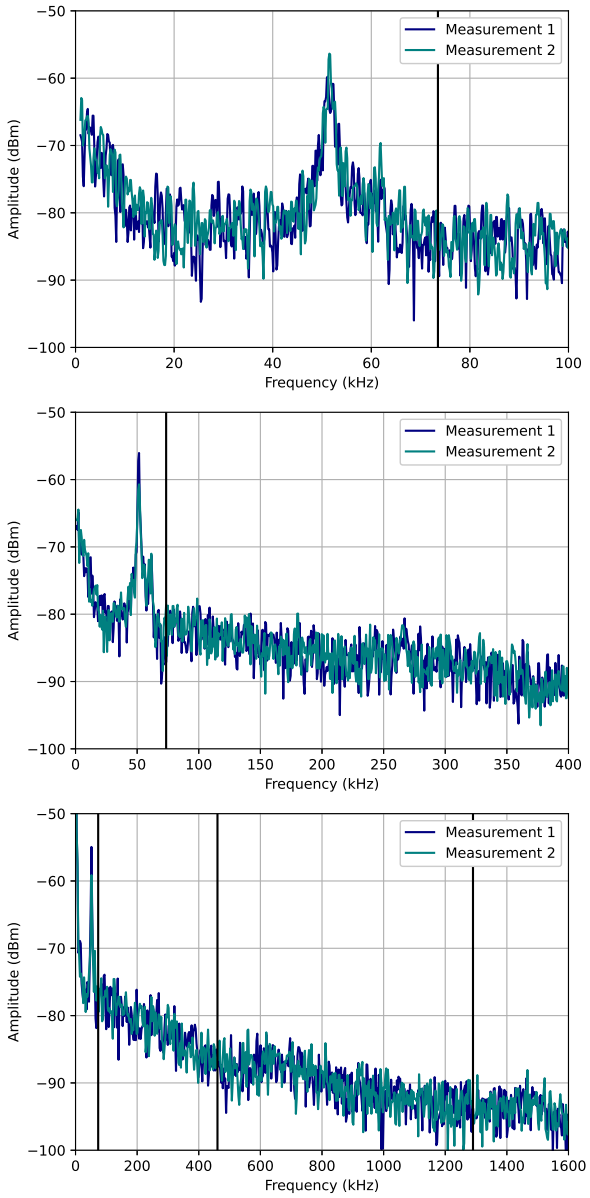

FIG. 8: Plot that gives the relation between the frequency (kHz) and amplitude (dBm) measured twice in the frequency domains $1-100$, $1-400$ and $1-1600$ kHz for the 100 μm cantilever. Additionally, the theoretically found resonance frequencies (see table II) are plotted.

Further research must figure out if the difference between practice and theory can be attributed to either the poor equipment, potential error in the values of parameters and potentially any other error present in this experiment or that actual theory contains mistakes. In addition to this, if the peaks do align with the theoretical values one could try and choose the frequency domain to be a small area around the higher-order peaks. This way, the now invisible, higher-order peaks can be analyzed. Due to the error between theoretical and practical values, this was not possible in this experiment.

The manual used for this experiment [4] specified spurious peaks will most likely occur in the measurements. In the measurements done in this paper, it is hard to spot these. However, one might be present at 270 kHz for the 200 μm cantilever. These spurious peaks could of course arise due to material imperfections or environmental noise. However, the most likely reasons are nonlinearities within the system that occur due to higher-order harmonics where combinations of frequencies create resonance or interaction between vibrational modes can lead to additional peaks. Using a better fiber tip, it is highly likely that a better view of these spurious peaks can be made and a more complete description and explanation of their behavior can be given.

Lastly, the 200 μm cantilever is mapped out along the length of the cantilever. The results can be seen in figure 9. From the last four values it can be observed that decreasing the length of cantilever decreases the amplitude. This aligns with the predictions since a smaller torque creates a smaller deflection/amplitude. However, this effect seems to halt below 75% usage. Below 75% the amplitude seems to stop decreasing. However, the measured amplitude can not be just noise, since the maximal value at the first resonance peak of 14 kHz is still higher for all the measurements than its surroundings. Therefore it is hard to give a specific reason for this phenomenon, it could be the case that there is some non-linear effect at such low amplitudes that only increases the amplitude significantly if a minimal torque is applied. To check if the findings from the last four values are correct a repeated experiment must be carried out with better equipment, especially a new and sharp fiber tip.

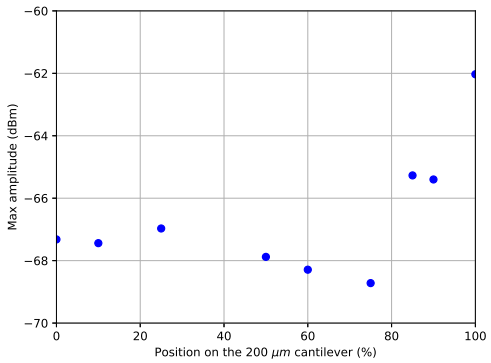

FIG. 9: Plot that gives the relation between the position (expressed as a percentage of the length) and the maximal amplitude (dBm) measured of the over the range $1-100$ kHz so that it contains the first resonance peak.

V. CONCLUSION

In this study, the resonance behavior of cantilever beams was studied and the optical cavity was characterized using a Fabry-Pérot interferometer. By analyzing the relationship between frequency, voltage, and amplitude, the responsivity of the piezo-stacks and the resonance frequencies of the beams were determined.

The responsivity measurements discovered that the piezo-stacks struggles at higher voltages, leading to significant uncertainties. Knowing this and choosing the right traces, a responsivity value of $R = 1.4 \pm 0.27 \ \frac{\mu m}{V}$ was obtained. Improvements in equipment could address this issue in future studies.

For the cutoff frequency of the piezo amplifier, we initially identified an incorrect range due to procedural errors. Correcting this, the cutoff frequency was determined to be $1125 \pm 125 \ Hz$. This large uncertainty show that there is a need for finer frequency scanning and potentially improved measurement techniques.

In the resonance analysis, the results deviated from the theoretical predictions. The errors are equal relatively which seems to imply that h might be inaccurate and actually be a smaller value.

Overall, this research provides valuable insights into the limitations of the current experimental setup and gives ideas for improvement. Future research could focus on addressing these limitations through better equipment, refined measurement techniques, and a more comprehensive error analysis to achieve greater accuracy and reliability in similar studies.

VI. APPENDIX

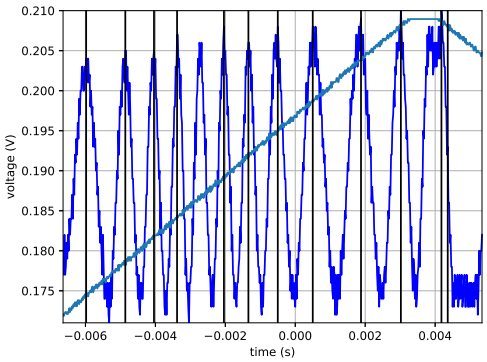

FIG. 10: Trace that gives the relation between the time (s) and voltage (V) for the 2 V. Here, the triangular wave is scaled to the current y-axis to show its shape. A algorithm is used to find the peaks with are displayed by black vertical lines.

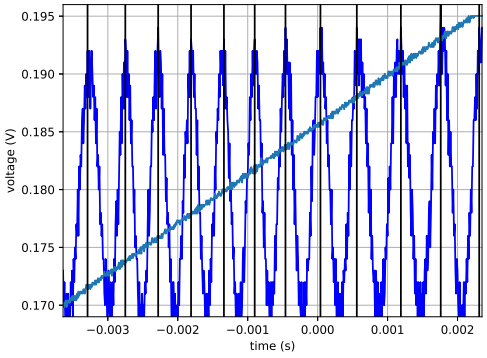

FIG. 11: Trace that gives the relation between the time (s) and voltage (V) for the 3 V. Here, the triangular wave is scaled to the current y-axis to show its shape. A algorithm is used to find the peaks with are displayed by black vertical lines.

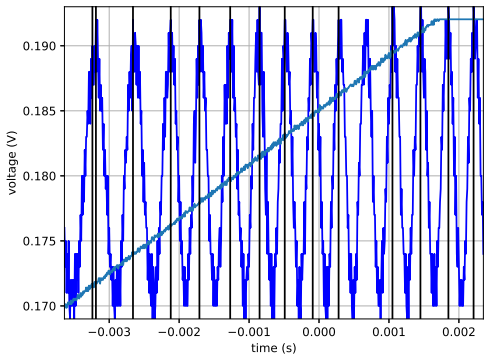

FIG. 12: Trace that gives the relation between the time (s) and voltage (V) for the 4 V. Here, the triangular wave is scaled to the current y-axis to show its shape. A algorithm is used to find the peaks with are displayed by black vertical lines.

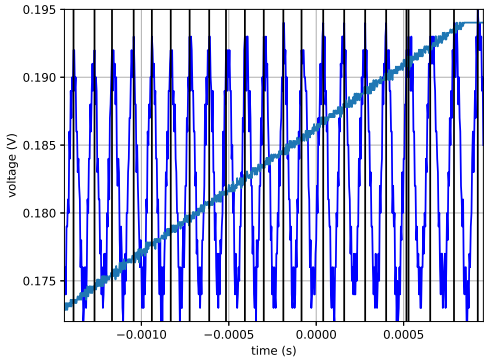

FIG. 13: Trace that gives the relation between the time (s) and voltage (V) for the 5 V. Here, the triangular wave is scaled to the current y-axis to show its shape. A algorithm is used to find the peaks with are displayed by black vertical lines.

[1] Michael Metcalfe. Applications of cavity optomechanics. *Applied Physics Reviews*, 2014.

[2] James M. Gere and Stephen P. Timoshenko. *Mechanics of Materials*. Van Nostrand Reinhold Company, New York, NY, second edition edition, 1984.

[3] Stan de Haas. Optomechanics. `https://github.com/StandeHaas/Optomechanics`, 2024.

[4] Characterization of a mechanical oscillator using fiber interferometry, 2023. Internal practicum document, last updated on August 1,2023.